J Fluoresc (2010) 20:153–161
DOI 10.1007/s10895-009-0533-4

ORIGINAL PAPER

Influence of Silver Nanoparticles on 2,3-Bis(Chloromethyl) Anthracene-1,4,9,10-Tetraone

Mahalingam Umadevi · N. A. Sridevi · A. S. Sharmila · Beulah J. M. Rajkumar · M. Briget Mary · P. Vanelle · T. Terme · O. Khoumeri

Received: 30 April 2009 / Accepted: 7 August 2009 / Published online: 25 August 2009

Abstract Size effect of silver nano particles on the photophysical properties of 2,3-bis(chloromethyl)anthracene-1,4,9,10-tetraone (BCMAT) have been investigated using optical absorption and fluorescence emission techniques. Silver NPs of different sizes have been prepared by two different methods. Quenching of fluorescence of BCMAT has been found to increase with decrease in the size of the silver NPs. Stern–Volmer quenching constants have also been calculated.

Keyword 2,3-bis(chloromethyl)anthracene-1,4,9,10-tetraone · Optical absorption · Fluorescence emission · Silver NP · Fluorescence quantum yield

Introduction

Anthraquinone is the most important quinone derivative of anthracene. Plants containing anthraquinones have been used as dyestuffs and purgatives [1]. Anthraquinone derivatives have various biochemical characteristics (bioactivities) and have the wide application for medicines, pesticides, etc. [2]. They are used principally in photographic dye chemicals, in medicine, as an antioxidant, in paints, varnishes, motor fuels, oils, pigments and in organic inhibitor. They play a vital role in paper industry as a catalyst to increase the pulp production yield and to improve the fiber strength through reduction reaction of cellulose to carboxylic acid [3, 4]. The anthraquinone derivative rhein is significantly antiseptic and is especially toxic to the enteric pathogen *Shigella dysenteriae* as well as to *Staphylococci* [5]. Moreover, many anthraquinones have been investigated for their anticancer potential [6].

The integration of nanotechnology with biology and medicine is expected to produce major advances in molecular diagnostics, therapeutics and bioengineering [7, 8]. Nanoscale metal particles have attracted significant attention because of their unusual size dependent optical and electronic properties. These nanomaterials have found potential applications in electronics, nonlinear optics, chemical and biochemical sensors, and in catalysis [9]. Due to surface plasmon excitation, NPs of silver, gold and copper may exhibit sharp electronic absorption bands in the visible region [10]. The size, shape and structure of NPs define their properties. Further the development of new procedures for the synthesis of nanomaterials with a well defined morphology is a very important research target [11]. The fluorescence of fluorophore might be enhanced or quenched due to the presence of nearby metallic NPs. The strength of the enhancement/quenching is influenced by many factors such as size and shape of the metal NPs, the orientation of the fluorophore dipole moments relative to the NPs, the radiative decay rate and quantum yield of the fluorophore. Lakowicz et al. reported that the quenching is usually observed if the fluorescence is located at a very

M. Umadevi (✉) · N. A. Sridevi · A. S. Sharmila
Department of Physics, Mother Teresa Women's University, Kodaikanal 624 102 Tamil Nadu, India
e-mail: ums10@yahoo.com

B. J. M. Rajkumar · M. B. Mary
Lady Doak College, Madurai, Tamil Nadu, India

P. Vanelle · T. Terme · O. Khoumeri
Laboratory of Radical Pharmaco-Chemistry, Faculty of Pharmacy, UMR CNRS 6264, University of the Méditerranée, 27 Bd Jean Moulin, 13385 Marseille Cedex 5, France

short distance (<5 nm) from the metal surface. When the fluorophore-metal distance is increased, both fluorescence quenching and enhancement have been observed [12].

Assembling fluorophore-metal NPs superstructures as a two or three dimensional architecture provides routes to design novel materials with tailored electrical, optical, lithographic, sensing and photochemical properties [13, 14]. Resonant energy transfer systems consisting of organic dye molecules and noble metal NPs have recently gained considerable interest in biophotonics as well as in materials science [15].

The biological importance of BCMAT molecule and silver NPs has prompted to the study the photo physical properties and the influence of size effect of silver NPs on this molecule. Interaction of a dye with the medium at the molecular level is reflected in its visible and fluorescence spectra. Fluorescence quenching is a technique to understand the interaction within the medium in view of the special role of surfaces of the nanoclusters in guiding and modifying physicochemical processes.

Recently our group has studied the effect of Ag NPs on 1,4-dihydroxy-2,3-dichloromethyl-9,10-anthraquinone [16]. C.D. Geddes et al. described the effect of Ag NPs on near by fluorophores [17, 18]. In the present study, optical absorption and fluorescence emission spectroscopic techniques have been employed to investigate the effect of silver NPs on 2,3-bis(chloromethyl)anthracene-1,4,9,10-tetraone (BCMAT) (Fig. 1).

Experimental

Reagents

Spectral grade methanol was obtained from SISCO laboratory and was used without further purification. Silver nitrate and sodium borohydride, purchased from Aldrich, were used as received. 2,3-bis(chloromethyl)anthracene-1,4,9,10-tetraone (BCMAT) was prepared in an original four step synthesis procedure from previously studied 1,4-dihydroxy-2,3-dimethylanthracene-9,10-dione. The 2,3-bis(chloromethyl)anthracene-1,4,9,10-tetraone was prepared in a four-step synthesis procedure from previously studied 1,4-dihydroxy-2,3-dimethylanthracene-9,10-dione [16]. After the oxidation of this last compound using lead acetate in toluene [19], the 2,3-dimethylanthracene-1,4,9,10-tetraone was brominated to give the unexpected 2,3-bis(bromomethyl)-1,4-dihydroxyanthracene-9,10-dione. An halogen exchange reaction using lithium chloride in THF, followed by another oxidation step with lead acetate in toluene [19] were necessary to form the desired 2,3-bis(chloromethyl) anthracene-1,4,9,10-tetraone. Doubly distilled water was used throughout.

Procedure

The silver NPs used in this study were synthesized by two different methods.

In the first method silver sol were prepared according to the following method. In brief 4 ml of silver nitrate solution (0.6 mM) was added drop wise to 25 ml of sodium borohydride solution (1.2 mM) with vigorous stirring. It was repeated for different volume of sodium borohydride (8, 12 and 16 ml) at constant volume of silver nitrate solution (25 ml). Both the solutions were chilled to ice temperature.

In the second method, the reduction of silver nitrate in boiling solution by addition of sodium citrate was employed. This method simply consists of addition of 1 ml of 1% sodium citrate solution to a 50 ml of boiling solution of silver nitrate and keeping it boiling for different times 90, 110, 130, 150 and 170 min.

The concentration of BCMAT in methanol was 0.01 mM. For the effect of silver NPs on BCMAT, BCMAT in methanol and silver sol have been taken in 1:1 volume ratio.

Fluorescence quantum yield

The relative fluorescence quantum yield (ϕ_{rel}) [20] of the sample in terms of the reference sample (ϕ_o) is $\phi_{rel} = \left(\frac{F}{F_o}\right)\left(\frac{OD_o}{OD}\right)\left(\frac{n}{n_o}\right)^2 \phi_o$ where F and F_o are the integrated fluorescence intensities, OD and OD_o are the optical densities and n and n_o are the refractive indexes for BCMAT in methanol and for 1,4-dihydroxy-2,3-dimethyl-9,10-anthraquinone (ϕ_o=0.0283) [21] in methanol respectively. In the present case the fluorescence quantum yield of BCMAT in methanol was found to be 0.0039.

Apparatus

Optical absorption spectra were recorded using a (Shimadzu UV-1700 pharmaspec) UV-Visible spectrophotometer. Elico Spectrofluorimeter SL174 was used to record fluorescence spectra. For fluorescence measurements the excitation wavelength was 500 nm. The spectra were recorded at room temperature.

Results and discussion

a) Silver nanoparticle size determination

Gustav Mie was the first to provide an explanation on the dependence of color on the metal particle size [22]. Surface plasmon resonance can be thought of as the collective oscillation of the conduction band electrons in

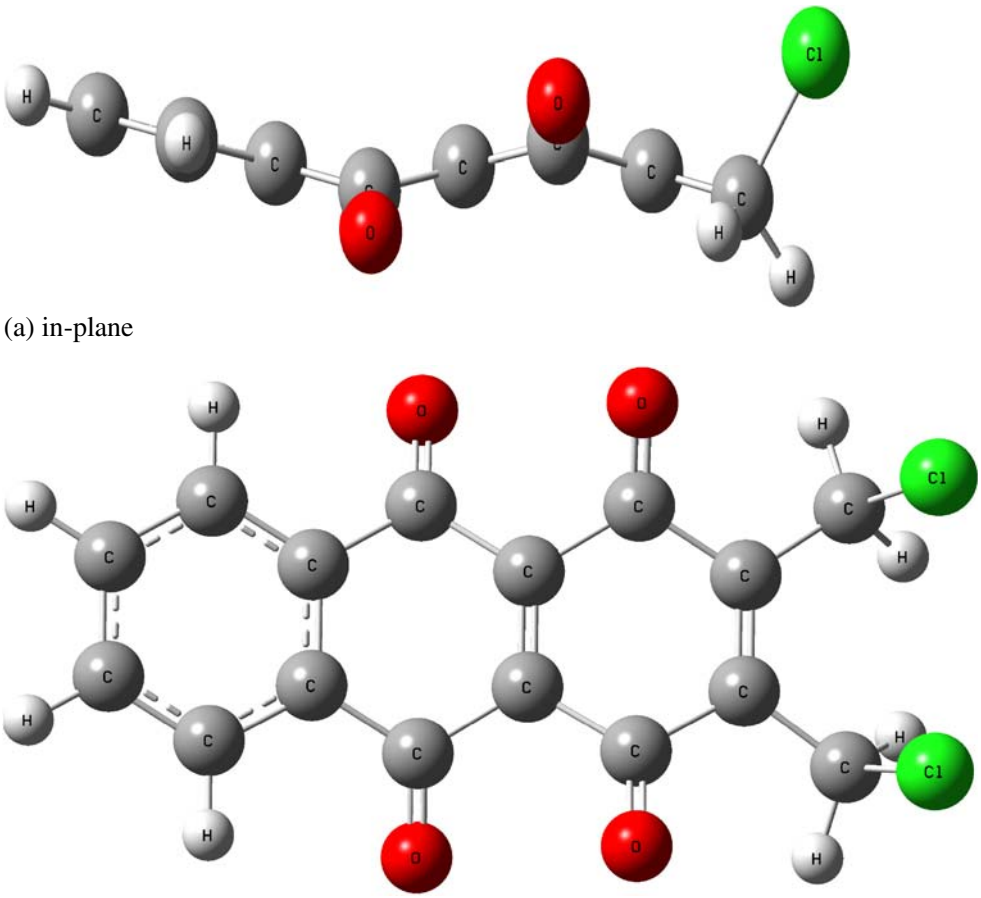

Fig. 1 In-plane (**a**) and out-of-plane (**b**) structure of BCMAT

(a) in-plane

(b) out-of-plane

the metals. This is due to the small size of the particle and surface property and is not exhibited by individual atoms or bulk materials. When the size of the particle is less than one tenth of the wavelength of the incident light, the electric fields can be assumed as spatially constant and only the temporal variation is taken into account. This state is called the quasi-static regime. Conduction bands electrons of alkali and noble metals interact strongly with the visible range of the electromagnetic waves. The incoming electric field of the electromagnetic wave induces a polarization of the electron with respect to the heavy ionic nucleus. The net charge difference is felt only at the surface (surface as defined by depth of penetration of the electromagnetic wave), which, it compensates with a restoring force in the form of a dipolar oscillation of the surface electrons in the same phase [23]. However when the size of the particle is comparable to their skin depth, all the electrons in the particle resonates, resulting in strong absorption of the particular wavelength. Since skin depth is dependent on the wavelength of the incident wave, particles of different sizes resonate at different wavelengths. This gives rise to different colors of silver colloid. The color of the colloid depends not just on the particle size, but also on the shape, the refractive index of the surrounding media and the separation between the particles. A change in any of these parameters will result in the quantifiable shift in the surface plasmon resonance absorption peak [24].

The optical properties of dispersions of spherical particles with a radius R can be predicted by Mie theory [22], through expression for the extinction cross section C_{ext}. For very small particles with a frequency dependent, complex dielectric function, $\varepsilon = \varepsilon' + i\varepsilon''$, embedded in a medium of dielectric constant ε_m this can be expressed as

$$C_{ext} = \frac{24\pi^2 R^3 \varepsilon_m^{3/2}}{\lambda} \frac{\varepsilon''}{(\varepsilon' + 2\varepsilon_m)^2 + \varepsilon''2} \quad (1)$$

The origin of the strong color changes displayed by small particles lies in the denominator of equation which predicts the existence of an absorption peak when

$$\varepsilon' = -2\varepsilon_m \quad (2)$$

In a small metal particle, the dipole created by the electric field of light induces a surface polarization charge which effectively acts as a restoring force for the free electrons. The net result is that, when condition (2) is fulfilled, the long wavelength absorption by the bulk metal

is condensed into a small surface plasmon band. Using this Mie theory the radius of the silver NPs have been calculated (Table 1).

In the present case the absorption spectrum has a maximum in the range 390–450 nm, which is related to the plasmon band of the formed nanosized silver particles (Figs. 2 and 3). This absorption band results from interactions of free electrons confined to small metallic spherical objects with incident electromagnetic radiation. Electronic modes in silver NPs are particularly sensitive to their shape and size, leading to pronounced effects in the visible part of the spectrum. The observed plasmon band shows that the silver NPs are spherical in shape [25].

b) Optical absorption and fluorescence emission studies

Quenching of fluorescence

Figures 4, 5 and 6 show the absorption spectrum of BCMAT in methanol and absorption spectra of BCMAT in different sizes of silver NPs respectively. Absorption spectrum of BCMAT in methanol shows a broad band in the visible region from 400 to 600 nm. It also indicates vibrational features with peals at 471, 488, 529 and 580 nm. The spacing between the peaks are 737, 1,575 and 1,659 cm^{-1} respectively.

The surface plasmon of silver sol shows a maximum in the range 390–450 nm for different sizes of silver NPs. When BCMAT is added to the silver sol, the plasmon band of silver shifts towards higher wavelength except for 8:25 (volume of $AgNO_3$:$NaBH_4$) and 110 m (heating time) shifts to shorter wavelength and its absorbance value decreases. In all the cases the vibrational features of BCMAT were disappeared and the feature of surface plasmon peak dominates. Dampening and broadening of the surface plasmon band was evident as these molecules complexed with the silver surface. The damping of the silver plasmon band indicates the attachment the BCMAT molecule on the particle surface. The interaction of silver nano particles with BCMAT alters the electron density of the silver NPs, thereby directly affecting the absorption of the surface bound BCMAT as well as surface plasmon absorption band.

Using these spectral shifts we can measure the binding constants of BCMAT with silver NPs in the ground state. The association constant for the complexation between silver NPs and BCMAT were obtained by analyzing the absorption changes using Benesi–Hildebrand approach. The association constant of $K_{ass} = 8.86 \times 10^3\ M^{-1}$ in silver NPs prepared by first method, was obtained from the plot of [BCMAT]/ΔA_{500} vs 1/[Ag] (Fig. 7) where ΔA_{500} is the changes in absorbance of BCMAT with and without silver NPs at 500 nm and [Ag] is the concentration of silver. The high value of K_{ass} observed in these experiments suggests a strong association between the silver colloid and BCMAT.

Figures 4, 8 and 9 depict the fluorescence emission spectrum of BCMAT in methanol and the fluorescence emission spectra of BCMAT in different sizes of silver NPs prepared by two different methods respectively. The observed fluorescence quantum yield of BCMAT in different sizes of NPs has been reported in Table 1. Fluorescence emission spectrum of BCMAT in methanol shows a broad band in the visible region with vibrational features. It shows two peaks at 588 and 683 nm and two shoulders around 553 and 639 nm. The absence of new broad band in the fluorescence emission spectra reveals that the BCMAT bound to silver NPS failed to exhibit intermolecular interaction such as excimer/exciplex formation or if there is the formation of any trace of the excimer, it is also quenched by the metal.

Table 1 Photophysical properties of BCMAT in silver NPs

First Method			
S. No.	Volume of aqueous (ml) $AgNO_3$:$NaBH_4$	Particle size (diameter) (nm)	Quantum yield (φ_{rel})×10^{-4}
1	4:25	36	5.51
2	8:25	27	3.74
3	12:25	22	2.96
4	16:25	22	1.70
Second Method			
S. No.	Heating time (minutes)	Particle size (diameter) (nm)	Quantum yield (φ_{rel})×10^{-4}
1	90	68.4	9.80
2	110	69.2	1.58
3	130	70.4	8.51
4	150	71.2	2.22
5	170	72	1.47

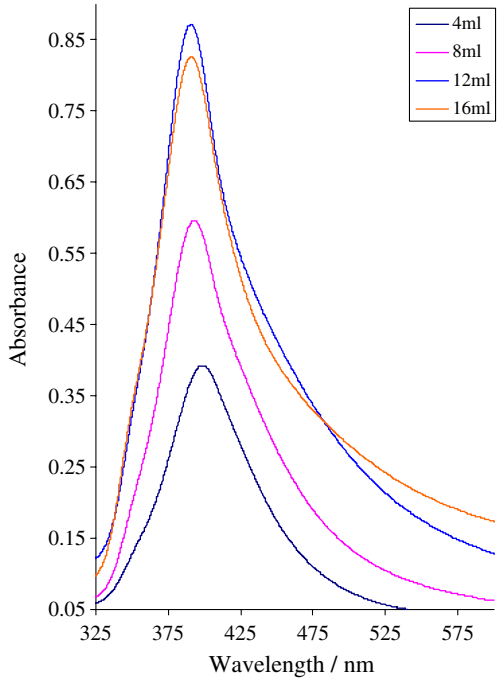

Fig. 2 Optical absorption spectra of silver NPs prepared by first method (4 ml–4 ml of $NaBH_4$ in 25 ml of $AgNO_3$)

When silver NPs are added to the BCMAT, the vibrational features of BCMAT are well resolved and the intensity was reduced. In the case of BCMAT in methanol, a strong intermolecular hydrogen bond is formed between OH group of methanol and C=O groups of BCMAT. But in silver NP environment the C=O groups of BCMAT

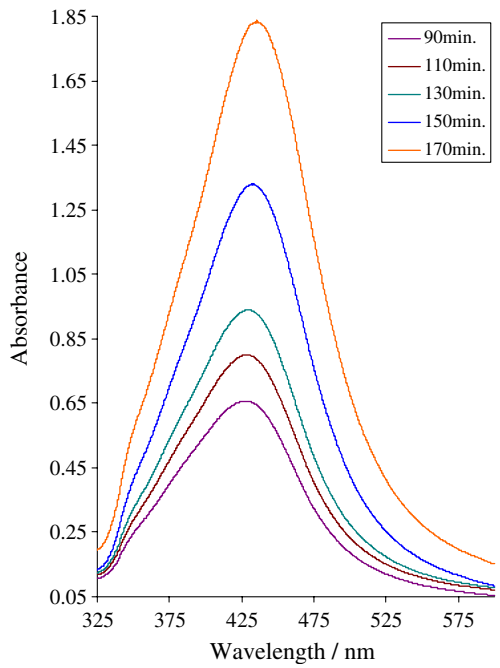

Fig. 3 Optical absorption spectra of silver NPs prepared by second method (90 min. (90 min)—heating time)

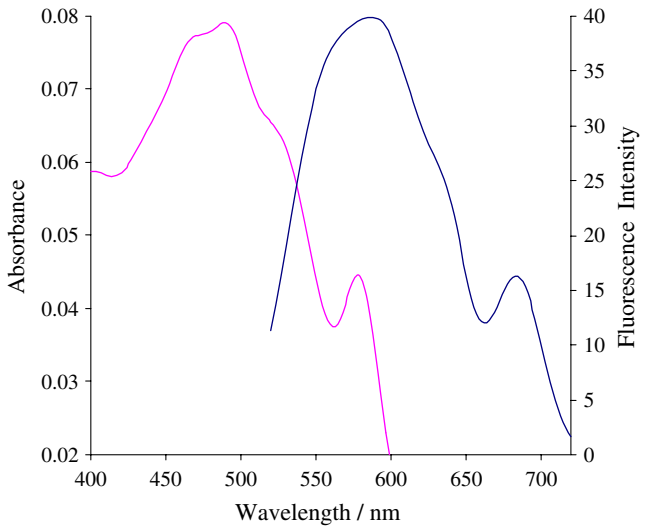

Fig. 4 Optical absorption and fluorescence emission spectra of BCMAT in methanol

adsorbed on the metal surface which break the intermolecular hydrogen bond. This strong intermolecular hydrogen bond mask the vibrational features of BCMAT which was absent in silver NP environment and leads to the observed features.

Excited state fluorophore behaves as an oscillating dipole, when these fluorophores are in close proximity to the metal surface, the rate of emission and the spatial distribution of the radiating energy will be modified. The electric field felt by the fluorophores are affect by the

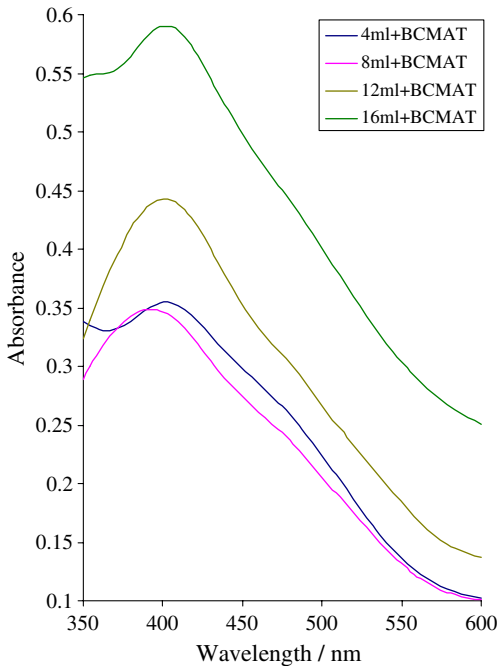

Fig. 5 Optical absorption spectra of BCMAT in silver NPs prepared by first method

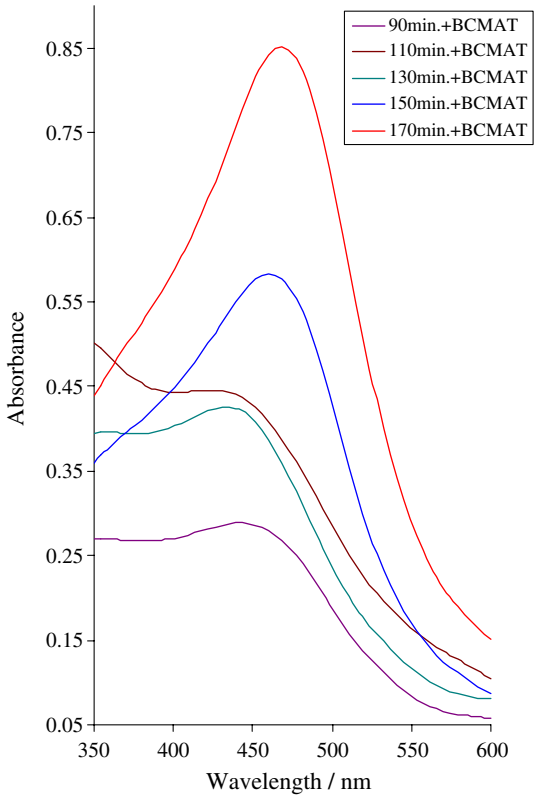

Fig. 6 Optical absorption spectra of BCMAT in silver NPs prepared by second method

interaction of the incident light with the nearby metal surface. These interactions can increase/decrease the field felt by the fluorophore and the increase/decrease the radiative decay rate [20] resulting in many desirable effects such as increased quantum yield and decreased lifetime. The radiative and non radiative rates depend on the size and shape of the NPs, the distance between the dye and the NPs the orientation of the molecular dipole with respect to the dye-NP axis and the overlap between the molecular emission spectrum with the NPs absorption spectrum.

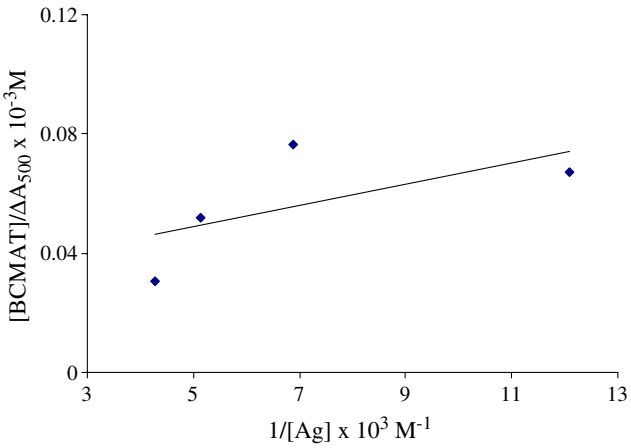

Fig. 7 Variation of [BCMAT]/ΔA_{500} versus 1/[Ag]

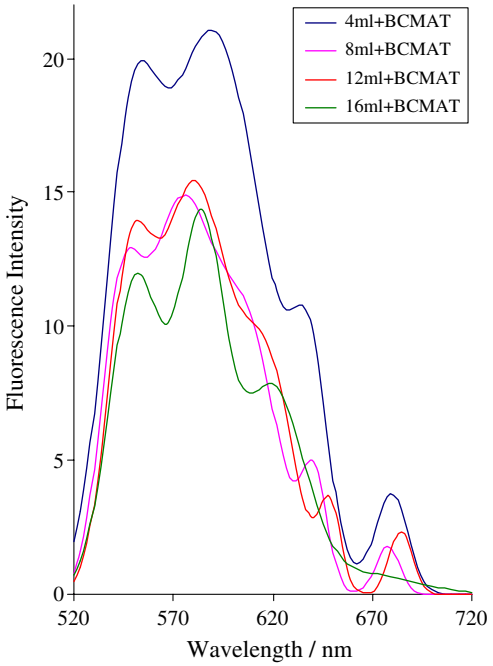

Fig. 8 Fluorescence emission spectra of BCMAT in silver NPs prepared by first method

In the present case quenching of fluorescence was observed for particles of different size. BCMAT molecules are attached to silver NPs via carbonyl groups. BCMAT is a non planar molecule that belongs to C_1 point group symmetry. The radii of NPs vary between 11 and 36 nm.

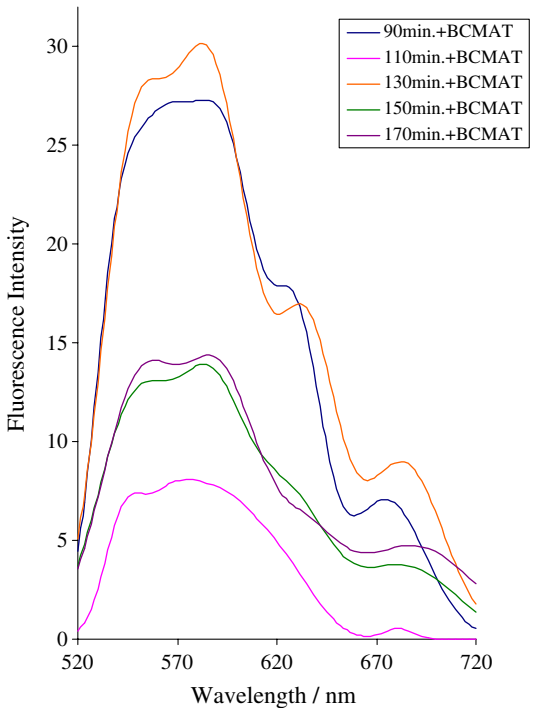

Fig. 9 Fluorescence emission spectra of BCMAT in silver NPs prepared by second method

The dipole moment of the π conjugated part of the molecule is oriented parallel to the silver NP axis and situated approximately 0.12 nm from the particles surface. The dipole moment of the C=O is oriented perpendicular to the silver NP axis (Scheme 1).

The energy transfer rate from NPs to the dye is governed by three factors, the Coulombic overlap integral, the position (surface plasmon frequency) and width (inverse surface plasmon lifetime) of the absorption spectrum of the NPs relative to those of dye. The size dependence of the energy transfer rate at large distanced for large NPs is determined entirely by the Coulombic overlap integral which in turn proportional to the quantum unit of dipole moment.

In the case of energy transfer from fluorophor to NPs, initially donor state of the system consists of an excited dye molecule and a NP in its ground state. The non radiative energy transfer from the dye to NP involves simultaneous de-excitation of molecule and collective excitation of compressible electron gas in the NP. The final acceptor state of the system consists of ground state dye molecule and a NP in its excited state. The rate of excitation energy transfer depends on the strength of Coulombic interactions and the spectral overlap between the emission spectrum of dye and absorption spectrum of NPs.

In the present case the overlap is between tail end of the absorption spectrum of NP and raising end of fluorescence emission spectrum of BCMAT and which is negligible. Therefore the rate of excitation energy transfer depends on spectral overlap is very weak. In this case the rate of excitation energy transfer depends mainly on the strength of Coulombic interactions between BCMAT and silver nano particles.

The influence of Coulombic interactions on the energy transfer has been studied in two different ways. First, the full Coulombic interactions between dye and NPs depends on the charge densities of dye and NPs. Second, the interaction within the dipole approximation, where the Coulombic interaction is approximated by the dipole interactions among the charge distribution of the dye and NPs. This dipole interaction mainly depends on the dipole moments of the dye and NPs and the distance between the dye and the NPs. The higher charge densities of BCMAT and the dipole moments of BCMAT and silver NPs are responsible for the energy transfer between BCMAT and silver NPs which leads to lower quantum yield.

Due to the electromagnetic coupling between the metal and the fluorophore, the metallic surface induces a strong quenching of molecular fluorescence. Weitz et al. [26] proposed a model to explain the NPs induced fluorescence quenching. The excitation of the electronic plasma resonance increases the absorption rate. Again, the molecular emission dipole excites the plasma resonance which increases the rate of radiative decay. In addition, the non-radiative decay provides damping effect when latter process increases, the quenching of fluorescence is observed. In the present case the excitation wavelength is 500 nm which does not coincide with the plasmon resonance peak of silver NPs and the silver NPs do not exhibit any fluorescence. Therefore the change in BCMAT fluorescence mediated by the electric near field due to silver NPs plasmon resonance is weak.

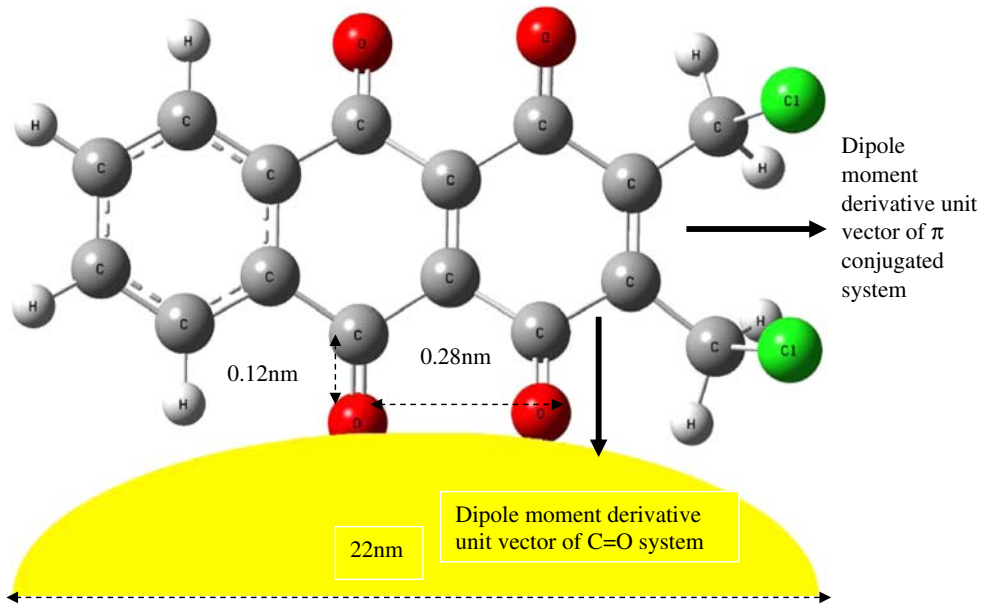

Scheme Orientation of BCMAT on silver NPs

Scheme 1 Orientation of BCMAT on silver NPs

Ditlbacher et al. [27] explained the changes of molecular fluorescence near a silver NP. When using fluorophore as local probes of the surface plasmon field of metallic NPs, in the close proximity of a metal, the fluorescence rate of the molecules is a function of the distance between the probe molecule and the metal surface. When in direct contact with the metal, the fluorescence of molecules is completely quenched.

The distance of closest approach of the probe molecules to the nano particles will change with the particle size. Thus the origin of the NP size dependence on the quenching process related to the absorption spectrum of the electronic states of the silver NPs. Due to the chemisorption of the BCMAT with the silver NP surface, the molecular orbitals of the BCMAT molecules are mixed with the metallic band states. Certain orbitals of BCMAT interact strongly with the silver NPs and are responsible for the chemisorption bond, while others are little affected by adsorption [28].

The size regime dependence of the silver NPs on the fluorescence quenching process can be explained by the structures of the NPs in terms of the size and surface chemistry. By changing the size of the NP using the same fluorophore, the interplay of size and surface effect on the structure of NPs can be realized.

The adsorption of the probe molecules on the NP surface is a function of the chemical composition, structure of the metal particle and nature of the solution. For a fixed set of solution parameters, the adsorption process is only influenced by the particle size. As the size of the particles decreases, there is an increasing contribution of the surface atoms. The increased surface area to volume ratio with progressive decrease in particle size can accommodate large number of fluorophore around silver NPs. Therefore small particles become efficient quenchers of molecular fluorescence than that of the larger ones. Silver NPs prepared by the first method shows that the fluorescence quantum yield decreases as the particle size increases. Since the small NPs adopt large number of BCMAT on the surface which leads to quenching of fluorescence.

When a donor molecule is placed in the vicinity of the conducting metal surface, resonant energy transfer takes place between the donor and acceptor. The probability of this Forster energy transfer depends on the overlap of the emission spectrum of the fluorophore with the absorption spectrum of the NPs. In the present case, this spectral overlap is negligible which leads to decrease in Forster radius and hence the rate of Forster energy transfers.

In the Gersten–Nitzan model [29] the radiative rate is derived by assuming Hertzian dipole emitters. Here the dipole for the entire system is considered by taking into account the intrinsic molecular dipole, the molecular dipole induced by the dipole field of the adjacent NPs, the dipole of the NPs driven by the dipole field of the adjacent NPs and the dipole of the NPs driven by the dipole field of the molecule. The resonant energy transfer of the molecular excitation is treated by calculating the absorption of the molecular dipole field at the position of the metal NPs. The observed decreased emission rate (lower quantum yield) is due to the phase shift between the BCMAT and the silver NP dipole leading to a destructive interference effect. This phase shift is caused by the complex nature of the silver dielectrics.

Both electron transfer and energy transfer processes are considered to be the deactivation pathways for excited fluorophores on the metal surface. The electron transfer mechanism is predominant for particle sizes of <5 nm as the particles do not exhibit any surface plasmon band in the visible region [30, 31]. In the present case silver NPs are larger than 5 nm, energy transfer dominates the quenching mechanism.

The medium/adsorbed molecules (electron donor or acceptor) can change markedly the effective concentration of electrons in the particle, resulting in a shift in the resonance and change in the width. Apart from this static dynamic effects related to the transfer of electrons from the Fermi surface to the adjacent levels of adsorbed molecules or the environment is also possible.

The surface plasmon efficiently acts as energy acceptor even at a distance of 1 nm between the probe molecules and the metal surface [32]. Metal NPs also have a continuum of electronic states and exhibit energy transfer behavior as excited state quenchers [28]. The observed changes in absorbance of the absorption spectrum and fluorescence intensity reflects the alteration of the electronic properties of the BCMAT chromophore as it binds to the silver NPs which act as a excited state quencher. The BCMAT has a high emission quantum yield in the absence of NPs, the dominant effect for the quenching of excited state of BCMAT in silver NPs may

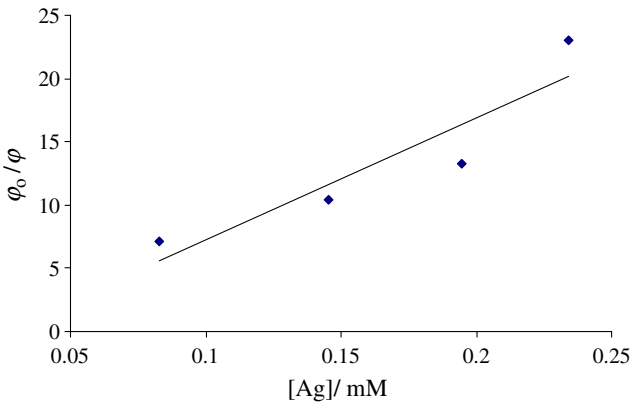

Fig. 10 Variation of φ_o/φ versus [Ag]

be due to radiative energy transfer to the metal surface. Fluorescence quenching may also result from a photo induced electron transfer process between the excited BCMAT and the silver NPs. The interaction with the dye and excited state surface reactions may lead to morphological changes of the silver NPs.

The Stern–Volmer equation accounting for both static and dynamic quenching is generally written as $\varphi_o/\varphi = 1 + K_{sv}[Ag]$ [20] where $K_{sv} = K_s + K_D$ where K_s and K_D are the static and dynamic quenching constants respectively, φ_o and φ are the fluorescence quantum yield of BCMAT in the absence and presence of quencher [Ag], respectively. There is no possibility of formation of static quenching complexes via attractive electrostatic interaction between fluorophore-quencher pairs collisional quenching is effectively possible. Figure 10 shows the plot of φ_o/φ vs silver concentration at constant BCMAT concentration. The plot is linear with $K_{sv} = 9.65 \times 10^4\ M^{-1}$ in silver NPs prepared by first method. The linearity of the Stern–Volmer plot indicates that only one type of quenching occurs in the system. In the presence of quencher the absorption spectrum of BCMAT remains unaltered in frequency. This indicates that static quenching does not occur. The Stern–Volmer quenching constant by silver NPs in the solution is very high indicating the presence of adsorption of the BCMAT on the quencher surface. The high quenching efficiency of the solution results from the larger surface area provided by the smaller NPs, which enhances their BCMAT adsorption capability.

Conclusion

Optical absorption and fluorescence emission techniques have been employed to study the photophysical properties of BCMAT on silver NPs. The process of fluorescence quenching of BCMAT by silver NPs indicate that the collisional quenching occurs and the quenching depends on the particle size of the silver NPs. The BCMAT molecules were adsorbed on the surface of the silver NP which leads to quenching of fluorescence.

References

1. Hirsikorpi M, Kamarainen T, Teeri T, Hohtola A (2002) Plant Sci 162:537
2. Yanzhu L, Min D, Ziwei S (1999) Tsinghua Sci Technol 4:4
3. Jahan MS (2001) Tappi J 84:61
4. Li Z, Li J, Kubes GJ (2002) J Pulp and Paper Sci 28:234
5. Brown JR, Imam SH (1984) Prog Mag Chem 21:196
6. Hua DH, Lou K, Havens J, Perchellet EM, Wang Y, Perchellet JP, Iwamoto T (2004) Tetrahedron 60:10155
7. Rosi NL, Mirkin CA (2005) Chem Rev 105:1547
8. Alivisatos P (2004) Nat Biotech 22:47
9. Kamat PV (2002) J Phys Chem B 106:7729
10. Merker M (1985) J Colloid Interface Sci 105:297
11. Pinna N, Weiss K, Sack-Kongehl H, Vogel W, Urban J, Pileni MP (2001) Langmuir 17:7982
12. Lakowicz JR (2005) Anal Biochem 337:171
13. Ivanisevic A, Mirkin CA (2001) J Am Chem Soc 123:7887
14. Imahori H, Norieda H, Yamada H, Nishimura Y, Yamazaki I, Sakata Y, Fukuzumi S (2001) J Am Chem Soc 123:100
15. Durbertret B, Calame M, Libchaber AJ (2001) Nat Biotech 19:365
16. Umadevi M, Vanelle P, Terme T, Rajkumar BJM, Ramakrishnan V (2008) J Fluoresc 18:1139
17. Aslan K, Holley P, Geddes CD (2006) J Mat Chem 16:2846
18. Geddes CD, Cao H, Gryczynski I, Gryczynski Z, Fang J, Lakowicz JR (2003) J Phys Chem A107:3443
19. Kerdesky FAJ, Ardecky RJ, Lakshmikantham MV, Cava MP (1981) J Am Chem Soc 103:1992
20. Lakowicz JR (1999) Principles of fluorescence spectroscopy, 2nd edn. Academic, New York
21. Umadevi M, Vanelle P, Terme T, Rajkumar BJM, Ramakrishnan V (2009) J Fluoresc 19:3
22. Bohren CF, Huffman DF (1983) Absorption and scattering of light by small particles. Wiley, New York
23. Link S, El-Sayed MA (2003) Annu Rev Phys Chem 54:331
24. Valmalette JC, Lemaire L, Hornyak GL, Dutta J, Hofmann H (1996) Analysis Magazine 24:m23
25. Mock JJ, Barbic M, Smith DR, Schultz DA, Schultz S (2002) J Chem Phys 116:6755
26. Weitz DA, Garoff S, Gersten JI, Nitzan A (1983) J Chem Phys 78:5324
27. Ditlbacher H, Krenn JR, Felidj N, Lamprecht B, Schider G, Salerno M, Leitner A, Aussenegg FR (2002) Appl Phys Lett 80:404
28. Huang T, Murray RW (2002) Langmuir 18:7077
29. Gersten J, Nitzan A (1981) J Chem Phys 75:1139
30. Ipe BI, Thomas KG, Barazzouk S, Hotchandani S, Kamat PV (2002) J Phys Chem 106:18
31. Fan C, Wang S, Hong JW, Bazan GC, Plaxco KW, Heeger AJ (2003) Appl Phys Sci 100:6297
32. Inacker O, Kuhn H (1974) Chem Phys Lett 27:317